GEOPHYSICAL RESEARCH LETTERS, VOL. 37, L04202, doi:10.1029/2009GL041465, 2010

Librational response of Enceladus

Nicolas Rambaux,[1] Julie C. Castillo-Rogez,[2] James G. Williams,[2] and Özgür Karatekin[3]

Received 22 October 2009; revised 30 November 2009; accepted 16 December 2009; published 24 February 2010.

[1] Physical librations could significantly contribute to Enceladus' geophysics through their influence on tidal stress. Therefore it is important to determine their behavior and the present paper is devoted to estimating Enceladus' libration in longitude. In a rotational model of Enceladus with no global ocean, we introduce the main perturbative terms of its orbital longitude and the tidal coupling. The main librations of Enceladus are related to indirect perturbations of the orbit of Enceladus by Dione (11 years and 3.7 years periods) with amplitudes of 933.4″ (1.14 km) and 676.6″ (827 m), respectively. These amplitudes are almost independent of the body's triaxiality. The third main libration is due to the direct gravitational attraction of Saturn and its period is equal to that of the mean anomaly of Enceladus with an amplitude between 93.1″ and 113.5″ (i.e., 112 and 139 m), depending on triaxiality. These amplitudes are consistent with the upper bound of 1.5° (6.6 km) inferred from observations with the Cassini-Huygens spacecraft. The nonrigid body libration amplitudes due to tidal coupling are negligible. Nevertheless, tidal dissipation induces a small phase shift up to 0.57° corresponding to a displacement of Enceladus' figure of 1 m along the moon's equator at the mean anomaly period. **Citation:** Rambaux, N., J. C. Castillo-Rogez, J. G. Williams, and Ö. Karatekin (2010), Librational response of Enceladus, *Geophys. Res. Lett.*, *37*, L04202, doi:10.1029/2009GL041465.

1. Introduction

[2] The Cassini-Huygens mission has detected an intensely active region at the South pole of Saturn's satellite Enceladus where the heat power is inferred to be between ~3 and 7 GW [*Spencer et al.*, 2006]. It has been suggested by *Hurford et al.* [2009] that physical libration might play an important role in the geological activity of Enceladus. The physical librations are oscillations of satellite's orientation around the otherwise uniform rotational motion of the body. Like the Earth's Moon, physical librations are generated by the departure from sphericity of the body and the orbital eccentricity, inclination and perturbations of the Keplerian orbit. At this time, the amplitude of the physical libration has not been measured although the Cassini Orbiter Imaging Science Subsystem [ISS] has provided an upper bound on the physical libration of 1.5° [*Porco et al.*, 2006]. *Comstock and Bills* [2003] investigated the response of Enceladus' librations at the orbital period and *Wisdom* [2004] studied a secondary resonance (based on pre-Cassini triaxiality determination). Recently *Hurford et al.* [2009] studied the relationship of tidal stress, consequent tidal dissipation and geological activity at the South pole with physical librations in longitude (oscillatory variations projected onto the equatorial plane). They focused on the physical libration acting at the orbital period, scanning a wide range of amplitudes (0 and 1.5°) and phases (0 and 180°), but without using a dynamical and interior model of the satellite. The purpose of this paper is to identify physical librations in longitude of Enceladus at different periods and to estimate their signatures for different assumptions on Enceladus' interior. For this study we assumed that Enceladus does not include an ocean, the presence of which at the global scale is a current matter of discussion [*Roberts and Nimmo*, 2008; *Tobie et al.*, 2008]. However, we considered a range of possible viscoelastic structures by varying the viscosity and rigidity for the icy shell.

[3] First, we present the dynamical model used for computing the libration in longitude affected by the main orbital perturbations, the tidal coupling, and the viscoelastic interior models. Then we describe the librational amplitudes and displacements for various geophysical models of Enceladus.

2. Dynamical Theory and Viscoelastic Models

2.1. Librational Equation

[4] If the dynamical figure of Enceladus were spherical, then the Saturnian torque would be zero and the body would rotate at a uniform rate. However, the Saturnian tidal potential and the centrifugal potential act on the figure of Enceladus by stretching its shape into a triaxial ellipsoid. For this reason, the Saturnian torque is non-zero and creates oscillations of the body around its rotation axis, the physical libration. Non-axisymmetric distribution of material in the interior and non-hydrostatic topography can also affect the triaxiality and the amplitude of the physical librations.

[5] The equations of rotation for bodies in synchronous spin-orbit resonance have been well developed for studies of the Earth's Moon [e.g., *Eckhardt*, 1981; *Williams et al.*, 2001]. The non-linear differential equations describing the rotational motion of a body in synchronous spin-orbit resonance might be linearized and give a good first order approximation for the libration angle [e.g., *Danby*, 1988, equation 14.3.6; *Williams et al.*, 2001, equation 17, and references therein]. The linearized equation is written as

$$\ddot{\gamma} + 3n^2\sigma\gamma = 3n^2\sigma(v - nt - \theta_0) \quad (1)$$

where γ is the angle of libration describing the oscillatory variations of the satellite's orientation (the long axis of the dynamical figure) θ projected onto the equatorial plane ($\theta = nt + \gamma + \theta_0$), n the mean motion, and θ_0 is a constant representing the initial value of θ located at the ascending

[1]IMCCE, UMR 8028, Observatoire de Paris, Université Pierre et Marie Curie, Paris, France.
[2]Jet Propulsion Laboratory, California Institute of Technology, Pasadena, California, USA.
[3]Royal Observatory of Belgium, Brussels, Belgium.

0094-8276/10/2009GL041465$05.00

This article was corrected on 03 FEB 2016. See the end of the full text for details.

Table 1. Main Terms in the Orbital Longitude of Enceladus From JPL Horizons Ephemeris[a]

i	Arg.	Period $2\pi/\omega_i$, days	Magnitude H_i, arcsec	Phase α_i, deg
1	ℓ	1.37	1954.84	27.83
2	ω_2	4035.63	933.43	−83.26
3	ϕ_4	1418.93	676.54	128.68

[a]Here ℓ is the mean anomaly, ω_2 is the orbital libration argument of the resonance Dione-Enceladus, and ϕ_4 is the proper pericenter of Dione (following notations of *Vienne and Duriez* [1995]).

node of Enceladus' orbit. The angle v is the longitude of Enceladus from the ascending node of the orbit and it is not the true anomaly as shown by *Danby* [1988]. The triaxiality parameter σ is equal to $(B - A)/C$, where $(A < B < C)$ are the unnormalized moments of inertia.

[6] For a Keplerian orbit, the difference $(v - nt - \theta_0)$ is known as the equation of the center and it can be expanded as a function of the mean anomaly ℓ [*Danby*, 1988]. However, the moon's orbit is not Keplerian due to perturbations by the other satellites. Then $v - nt - \theta_0$ can be expanded in a series, denoted as s, which will include terms corresponding to both periodic functions of ℓ and perturbations of the orbit of Enceladus away from its Keplerian form [e.g., *Vienne and Duriez*, 1995].

$$s = \sum_i H_i \sin(\omega_i t + \alpha_i) \tag{2}$$

H_i, ω_i, and α_i are respectively the magnitude, the frequency and the phase of the orbital periodicities, and the solution of equation (1) is simply

$$\gamma = A_0 \sin(\omega_0 t + \phi_0) + \sum_i \frac{\omega_0^2 H_i}{\omega_0^2 - \omega_i^2} \sin(\omega_i t + \alpha_i) \tag{3}$$

where $\omega_0 = n\sqrt{3\sigma}$ is the resonant frequency of this spin-orbit problem and A_0, ϕ_0 are two constants of integration.

2.2. Libration Equation With Dissipation

[7] Saturn produces not only a net torque on Enceladus but also deforms its surface. The tidal bulge raised by Saturn does not respond instantaneously and the time delay δt is a function of the satellite's interior viscoelastic properties. It is frequency dependent, $\delta t_i = \delta t(\omega_i)$, and will be described in section 2.4.

[8] The main tidal torque acting on Enceladus additional to equation (1) is the torque expressed as [*Williams et al.*, 2001, see equation 14]

$$T = -k_2 R^5 \frac{3GM^2}{a^6}(U_{11}U_{12}^* - U_{12}U_{11}^*), \tag{4}$$

where R is Enceladus' radius, k_2 the tidal Love number, G the gravitational constant, M the mass of Saturn, and $U_{ij} = (\frac{a}{r})^3 u_i u_j$, a and r are the semi-major axis and the radius vector between Saturn and Enceladus; here $a \sim r$. The u_i are the direction cosines along the moment of inertia principal axes with subscripts 1, 2, 3 corresponding to direction along A, B and C, respectively. The star indicates that the function U_{ij} is accounting for dissipation. Using the synchronous rotation of Enceladus, we neglect the square terms of u_2, u_3 and set $U_{11} \simeq U_{11}^* \simeq 1$ and $U_{12} = s - \gamma$. The expression of $U_{12}^* = s^* - \gamma^*$ is from a Fourier series expansion with the argument of each ith component developed in a Taylor series using each δt_i as shown by *Efroimsky and Williams* [2009]. The equation governing the libration in longitude is then a forced damped oscillator with the frequency-dependent damping coefficient λ_i defined by

$$2\lambda_i = \frac{3k_2R^3}{C}\frac{n^4}{Gm}\delta t_i, \tag{5}$$

where m is the mass of Enceladus. The librational angle has the form

$$\gamma = A_d \sin(\omega_d t + \phi_d)e^{-\lambda_d t} + \sum_i B_i \sin(\omega_i t + \alpha_i + \phi_i) \tag{6}$$

where the first term decays with time scale $1/\lambda_d$ where λ_d is the damping coefficient at the resonant frequency and its resonant frequency is $\lambda_d = \sqrt{\omega_0^2 - \gamma_d^2}$, slightly shorter with dissipation than without it. A_d and ϕ_d are new constants of integration. The periodic term of the particular solution γ is composed of the amplitude and phase shift

$$B_i = \sqrt{\frac{H_i^2(4\lambda_i^2\omega_i^2 + \omega_0^4)}{(\omega_0^2 - \omega_i^2)^2 + 4\lambda_i^2\omega_i^2}}, \quad \tan\phi_i = \frac{-2\lambda_i\omega_i^3}{(\omega_0^2 - \omega_i^2)^2 + 4\lambda_i^2\omega_i^2}. \tag{7}$$

2.3. Orbital Motion

[9] Our representation of the orbital motion of Enceladus is obtained from numerical ephemeris Horizons [*Giorgini et al.*, 1996]. From this ephemeris, we computed the true longitude of Enceladus. Then we expressed the longitude in the form of quasi-periodic series by using frequency analysis [*Laskar*, 1988, 2005]. The main terms in the longitude are listed in Table 1. The first term is the leading term of the equation of center corresponding to $2e \sin \ell$ where e is the eccentricity of the satellite and ℓ the mean anomaly of the satellite. The two last terms are related to the Dione-Enceladus resonance. They are the orbital libration argument of the Dione-Enceladus resonance ω_2 and the motion of the proper pericenter of Dione ϕ_4 (following notations of *Vienne and Duriez* [1995]). The initial time of the series is J2000 [*Giorgini et al.*, 1996]. Due to the short span of the ephemeris, the phase of ω_2 is reached with a precision of 2%.

2.4. Viscoelastic Models

[10] In this paper, we assumed that Enceladus is in hydrostatic equilibrium, differentiated into a rocky core and icy shell without a global ocean. The departure from hydrostaticity is small [*Porco et al.*, 2006]. We built interior models with an icy shell density of 1000 kg/m^3 and a core density ranging from 2700 kg/m^3 (mostly hydrated silicates) to 3500 kg/m^3 (anhydrous rock). The resulting ice shell thickness varies between 73 km and 95 km. The triaxiality of Enceladus is calculated from spherical harmonic degree 2 gravitational coefficients C_{22} and C_{20} for the assumed equilibrium ellipsoidal distortion of the satellite [*Hubbard and Anderson*, 1978]. The corresponding σ ranges from

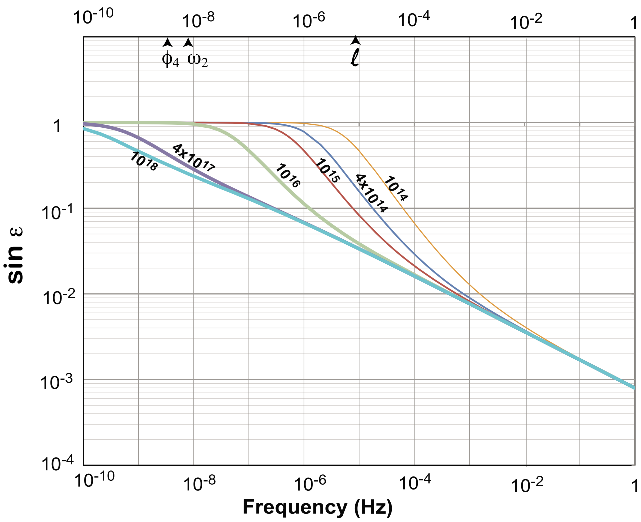

Figure 1. Ice dissipation spectrum computed with the Andrade model for $m = 0.33$ and $\beta = 10^{-12}$ and various ice viscosities (indicated in Pa s). The arrows indicate the frequencies of the three librations in longitude considered in this study.

0.0151 to 0.0183. For a homogeneous model, the triaxiality σ would be equal to 0.0231. In the following calculation we used a value of $\sigma = 0.0168$ corresponding to a shell thickness of 82 km, a shell density of 1000 kg/m^3 and a rock density of 3000 kg/m^3.

[11] *Efroimsky and Lainey* [2007] reviewed the literature on attenuation in planetary objects and materials and stressed the inconsistency of the Maxwell model with experimental measurements and geophysical observations. The authors noted that the attenuation spectrum of planetary material can be described by an "elbow-shape." *Castillo-Rogez and McCarthy* [2010] indicated that this "elbow-shaped" spectrum is also applicable to ices and that it is best fitted by the geophysical model of *Andrade* [1910] (see Figure 1). The Andrade function depends on the steady-state shear viscosity η and unrelaxed shear modulus G of the material [e.g., *Gribb and Cooper*, 1998]

$$\sin \epsilon_i = \frac{J''}{(J'^2 + J''^2)^{1/2}} \quad (8)$$

where ϵ_i is the frequency-dependent tidal phase lag, and

$$J'' = (\eta\omega_i)^{-1} + \beta\omega_i^{-m} \sin\left(\frac{m\pi}{2}\right)\Gamma(m+1)$$
$$J' = (G)^{-1} + \beta\omega_i^{-m} \cos\left(\frac{m\pi}{2}\right)\Gamma(m+1) \quad (9)$$

where, Γ is the Gamma function, the exponent m determines the slope of the response as a function of frequency in the transient regime. Fits of the transient response of polycrystalline ice deforming in the grain-boundary sliding regime, relevant to Enceladus' conditions of stress and temperature, yielded $m \sim 0.3–0.38$ [e.g., *Castelnau et al.*, 2008]. The parameter β characterizes the nature, the density, and the distribution of the defects involved in the internal friction and determines the amplitude of the relaxation. If β is negligible in equation (9), then the Andrade model tends toward the Maxwell model. A value of β in the $10^{-11}–10^{-13}$ range is consistent with laboratory measurements [e.g., *Castillo-Rogez and McCarthy*, 2010]. For the sake of simplicity, we assumed β is constant throughout the icy shell.

[12] Unlike the Maxwell model, the Andrade model can account for the ice anelastic response when forced at periods smaller than the material's Maxwell time, $\tau = \eta/G$. For viscosities $\geq 4 \times 10^{14}$ Pa s the satellite's tidal response is dominated by the ice anelastic behavior at the orbital period, and by the ice steady-state (viscous) behavior at longer libration periods.

[13] For a multilayered interior model, we computed the compliance (response of each viscoelastic layer to stress) and the complex Love number k_2 (response of the whole body to tidal stress computed from the integration of spheroidal oscillations in the multilayered model [*Tobie et al.*, 2005; *Castillo-Rogez et al.*, 2007]). For this study we assumed that (1) the thickness of each layer is constant, although variations of icy shell viscoelasticity might exist [*Smith*, 2008] and (2) the dissipation rate is averaged over the surface of the body. The ice steady-state viscosity ranges from 10^{12} Pa s to 10^{17} Pa s in the icy shell; the lower bound corresponds to warm ice with a few percent melt, while the dissipation becomes negligible, at all relevant frequencies, if the viscosity is greater than the upper bound. We assumed that the rocky core has a high viscosity of 10^{21} Pa s as suggested by *Roberts and Nimmo* [2008]. This results in little contribution from the core to the global tidal dissipation. We found a range of k_2 between $6. \times 10^{-4}$ and 0.013. The lower bound corresponds to a rigid model in which η is equal to or greater than 10^{17} Pa s. The upper bound corresponds to a very dissipative case assuming the ice viscosity is 10^{12} Pa s and $\beta = 10^{-12}$. From this calculation we inferred the time delay $\delta t_i = \epsilon_i/\omega_i$ [*Efroimsky and Williams*, 2009].

3. Results and Discussion

3.1. Physical Libration: Non-dissipative Case

[14] The libration amplitudes for the non-dissipative dynamical model defined in section 2.1 are listed in Table 2. The main libration corresponds to the orbital libration argument of Dione-Enceladus ω_2, then the proper pericenter of Dione ϕ_4, and finally the mean anomaly. The short-period libration has a small amplitude because its frequency $n = 4.58$ rad/d is higher than the resonant frequency $\omega_0 \sim 1.03$ rad/d leading to an amplitude ratio smaller than 1. In contrast, at longer periods where $\omega_0 \gg \omega_i$ the librational amplitude is nearly equal to the magnitude of the coupling H_i. As a consequence, for Enceladus with 1.2 m/arcsec on the equator, the amplitude of the libration increases with the period so that the largest libration term has a period of 11 yr

Table 2. Main Physical Librations of Enceladus for a Non-dissipative Case for $\sigma = 0.0168$.

i	Arg.	Period $2\pi/\omega_i$, days	Amplitude, arcsec	Phase α_i, deg
1	ℓ	1.37	−103.73	27.83
2	ω_2	4035.64	933.44	−83.26
3	ϕ_4	1418.93	676.56	128.68

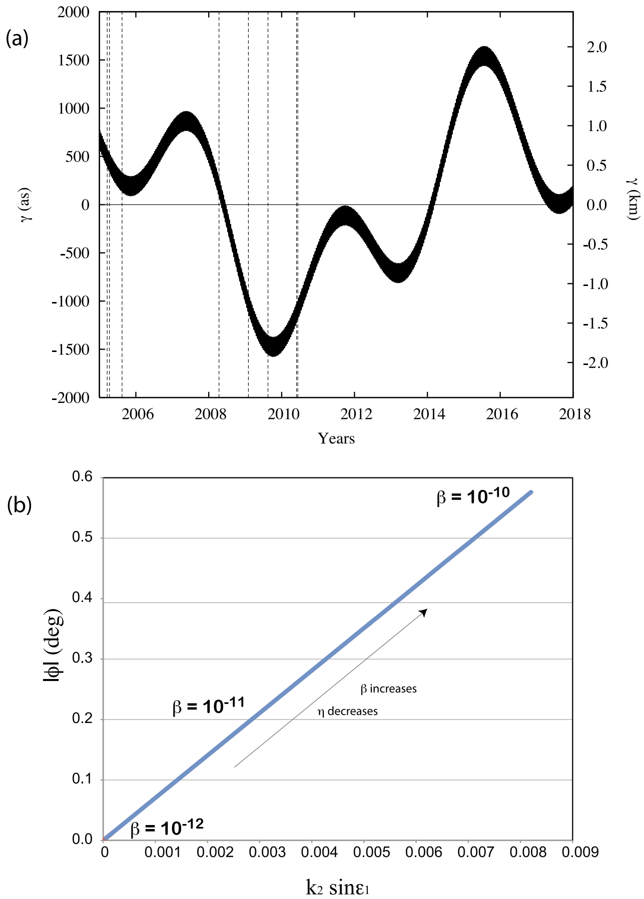

Figure 2. (a) Physical libration of Enceladus for the 2005–2018 period in arcseconds (as) and kilometers (km). The curve presents the three main librations. The thickness of the curve is due to the libration at the orbital period. The vertical lines indicate the times of past and planned Cassini flybys at Enceladus. (b) Absolute value of the shift angle as a function of $k_2 \times \sin\epsilon_1$ at the orbital period. These parameters have been computed under several assumptions on the value of β and for a range of viscosity of 10^{12}–10^{17} Pa s; these two parameters are almost independent of each other. The range of values for $k_2 \times \sin\epsilon_1$ corresponds to a global dissipation power between 0 and ~22 GW.

with an amplitude of 1.14 km, then a 3-yr period libration has an amplitude of 827 m, and finally the orbital period oscillation has a 127 m amplitude. Varying the triaxiality, i.e., the mass distribution, we find constant amplitudes for the long-period librations and an amplitude ranging between 112 and 139 m for the orbital period libration. For the homogeneous case, we obtained an amplitude equal to 178 m.

[15] The librational phase is related to the phase of orbital excitation. The librational and orbital phases coincide for frequencies smaller than the resonant frequency (i.e., for arguments ω_2 and ϕ_4) and differ by π for frequencies greater than the resonant frequency, i.e., ℓ (in Table 2, we fix the phase and use negative sign for the amplitude). The temporal evolution of the physical libration of Enceladus is presented in Figure 2. Figure 2a shows the physical libration. The thickness of the line is due to the libration of 103.73″ amplitude at the 1.37 day period. The vertical lines show the Cassini flybys dates. We note that in 2010 the physical libration is expected to be near an extremum.

3.2. Consequences of the Tidal Dissipation

[16] Now, we estimate the impact of tides on the libration and orientation of Enceladus. The ratio p of the amplitude of the dissipative to the amplitude of the non-dissipative libration is

$$p = 1 - 2\lambda_i^2\omega_i^4 \frac{(2\omega_0^2 - \omega_i^2)}{(\omega_0^2 - \omega_i^2)^2\omega_0^4} \tag{10}$$

approximated to second-order in λ_i. As a consequence, the amplitude for the dissipative model is the same as the amplitude for the non-dissipative case at second-order in λ_i. The greatest effect is observed for the short-period term where $\epsilon_1 = 37.5°$, $k_2 = 0.013$ with an increase of the libration amplitude by 0.005″, which is still relatively small.

[17] In absence of internal dissipation, the phase of the physical libration is equal to the phase of the excitation or the phase plus π depending on the sign of $\omega_0^2 - \omega_i^2$. Due to dissipation, the satellite's librational phase is shifted backward by an angle $|\phi_i|$, see equation (7). Figure 2b shows the relationship of the phase shift to internal dissipation expressed through $k_2 \sin \epsilon_1$.

[18] The solution space in Figure 2b covers a wide range of viscosity of the icy shell (see section 2.4). The upper bound corresponds to dissipative models characterized by a small viscosity as low as 10^{12} Pa s, whereas the bottom limit corresponds to a non-dissipative model. Moreover, by using *Wisdom* [2004] formulation, we infer that the forced librations contribute only ~6% to Enceladus' global tidal heating.

[19] The displacement along the Enceladus equator could be measured from observations of Enceladus' geological landmarks obtained when the satellite is at different points along its orbit. The short-period term at ℓ is the most sensitive to the dissipation. At phase 0 or π, the influence of dissipation on libration is extreme: the quantity $\sin(\omega_1 t + \alpha_1)$ is equal to zero and the size of the dissipation effect becomes $\pm B_1 \sin\phi_1$. Table 2 and Figure 2b indicate that the maximum dissipation phase shift $|\phi_i|$ is equal to 0.57° and the displacement of the orientation figure is 1.26 m with respect to a non-dissipative case.

4. Conclusion

[20] In this paper we developed the formalism for the longitudinal oscillations of Enceladus. We introduced the main perturbative terms of the orbit, especially the terms arising from the orbital resonant libration of Dione-Enceladus.

[21] We found that the three main librational oscillations have periods of 11 years, 3.7 years and 1.37 days. The long period librations are due to the Enceladus-Dione resonance, with the largest libration amplitude of 1.14 km almost independent of the triaxiality value. The 1.37 day oscillation has an amplitude of 127 m for a triaxiality of 0.0168. We assessed the influence of the triaxiality on the amplitude of that libration by varying the core radius and density of the icy shell, i.e., distribution of mass inside the two-layer model. For the stratified endmembers, the amplitude of

the libration at 1.37 days varies from 112 to 139 m. For a homogeneous model, we obtained an amplitude equal to 178 m. The tidal dissipation does not influence the amplitude of the librations.

[22] These libration amplitude estimates fall below the upper detection limit inferred from Cassini Imaging [*Porco et al.*, 2006], equal to 1.5° (6.6 km). Future flybys of Enceladus by the Cassini Orbiter offer the opportunity to refine these measurements. Especially, Enceladus will reach a physical libration angle up to 1100″ (1.3 km) in April–May 2010. These results also stress the importance of accounting for the physical librations of 3 and 11 year periods when fitting and interpreting shape data, in order to avoid confusion with other processes affecting the shape, such as non-synchronous rotation.

[23] We also estimated the displacement of orientation along Enceladus' equator in the presence of tidal dissipation. For a range of viscoelastic models we found phase shift angles as large as 0.57° corresponding to displacements up to 1.26 m.

[24] The displacement may be inferred from gravity measurements, tracking of surface landmarks, and/or altimetry measurements. However such a determination requires several close flybys for different positions of Enceladus along its orbit, as may be achievable with a dedicated orbiter [*Russell and Strange*, 2009]. In the meantime, we hope that upcoming flybys by the Cassini orbiter will help to better constrain the orientation of the figure axis of Enceladus.

[25] **Acknowledgments.** NR thanks Philippe Robutel for fruitful discussions. NR and OK acknowledge the French Enceladus working group. We thank M. Efroimsky for his constructive reading. Part of this work has been conducted at the Jet Propulsion Laboratory, California Institute of Technology, under a contract with the National Aeronautics and Space Administration. Copyright 2009. All rights reserved. Government sponsorship acknowledged. We also thank Bonnie Buratti, Sharon Chapman, and the JPL Science Visitor and Colloquium Program.

References

Andrade, E. N. D. C. (1910), On the viscous flow in metals, and allied phenomena, *Proc. R. Soc. London, Ser. A*, *84*, 1.

Castelnau, O., P. Duval, M. Montagnat, and R. Brenner (2008), Elastoviscoplastic micromechanical modeling of the transient creep of ice, *J. Geophys. Res.*, *113*, B11203, doi:10.1029/2008JB005751.

Castillo-Rogez, J. C., and C. McCarthy (2010), Physics of dissipation in ice and icy bodies, in *The Science of Solar System Ices*, edited by M. Gudipati and J. Castillo-Rogez, Springer ASSL, in press.

Castillo-Rogez, J. C., D. L. Matson, C. Sotin, T. V. Johnson, J. I. Lunine, and P. C. Thomas (2007), Iapetus' geophysics: Rotation rate, shape, and equatorial ridge, *Icarus*, *190*, 179.

Comstock, R. L., and B. G. Bills (2003), A solar system survey of forced librations in longitude, *J. Geophys. Res.*, *108*(E9), 5100, doi:10.1029/2003JE002100.

Danby, J. M. A. (1988), *Fundamentals of Celestial Mechanics*, Willman-Bell, Richmond, Va.

Eckhardt, D. H. (1981), Theory of the libration of the moon, *Moon Planets*, *25*, 3.

Efroimsky, M., and V. Lainey (2007), Physics of bodily tides in terrestrial planets and the appropriate scales of dynamical evolution, *J. Geophys. Res.*, *112*, E12003, doi:10.1029/2007JE002908.

Efroimsky, M., and J. G. Williams (2009), Tidal torques: A critical review of some techniques, *Celestial Mech. Dyn. Astron.*, *104*, 257.

Giorgini, J. D., et al. (1996), JPL's on-line solar system data service, *Bull. Am. Astron. Soc.*, *28*, 1158.

Gribb, T. T., and R. F. Cooper (1998), Low-frequency shear attenuation in polycrystalline olivine: Grain boundary diffusion and the physical significance of the Andrade model for viscoelastic rheology, *J. Geophys. Res.*, *103*, 27,267.

Hubbard, W. B., and J. D. Anderson (1978), Possible flyby measurements of Galilean satellite interior structure, *Icarus*, *33*, 336.

Hurford, T. A., B. G. Bills, P. Helfenstein, R. Greenberg, G. V. Hoppa, and D. P. Hamilton (2009), Geological implications of a physical libration on Enceladus', *Icarus*, *203*, 541.

Laskar, J. (1988), Secular evolution of the solar system over 10 million years, *Astron. Astrophys.*, *198*, 341.

Laskar, J. (2005), Frequency map analysis and quasi periodic decompositions, in *Hamiltonian Systems and Fourier Analysis*, edited by D. Benest, C. Froeschler, and E. Lega, Cambridge Sci., Cambridge, U. K.

Porco, C. C., et al. (2006), Cassini observes the active south pole of Enceladus, *Science*, *311*, 1393.

Roberts, J. H., and F. Nimmo (2008), Tidal heating and the long-term stability of a subsurface ocean on Enceladus, *Icarus*, *194*, 675.

Russell, R. P., and N. J. Strange (2009), Cycler trajectories in planetary moon systems, *J. Guidance Control Dyn.*, *32*, 143.

Smith, D. E. (2008), Viscous relaxation of craters on Enceladus, M.S. dissertation, 76 pp., Univ. of Ariz., Tucson.

Spencer, J. R., et al. (2006), Cassini encounters Enceladus: Background and the discovery of a south polar hot spot, *Science*, *311*, 1401.

Tobie, G., A. Mocquet, and C. Sotin (2005), Tidal dissipation within large icy satellites: Applications to Europa and Titan, *Icarus*, *177*, 534.

Tobie, G., O. Čadek, and C. Sotin (2008), Solid tidal friction above a liquid water reservoir as the origin of the south pole hotspot on Enceladus, *Icarus*, *196*, 642.

Vienne, A., and L. Duriez (1995), TASS1.6: Ephemerides of the major Saturnian satellites, *Astron. Astophys.*, *297*, 588.

Williams, J. G., D. H. Boggs, C. F. Yoder, J. T. Ratcliff, and J. O. Dickey (2001), Lunar rotational dissipation in solid body and molten core, *Astrophys. J.*, *106*, 27933.

Wisdom, J. (2004), Spin-orbit secondary resonance dynamics of Enceladus, *Astrophys. J.*, *128*, 484.

J. C. Castillo-Rogez and J. G. Williams, Jet Propulsion Laboratory, California Institute of Technology, Mail Stop 183-401, Pasadena, CA 91109, USA.

Ö. Karatekin, Royal Observatory of Belgium, 3 Avenue Circulaire, B-1180 Brussels, Belgium.

N. Rambaux, IMCCE, UMR 8028, Observatoire de Paris, Université Pierre et Marie Curie, F-75014 Paris, France. (nicolas.rambaux@imcce.fr)

Erratum

In the originally published version of this article, several instances of text appeared incorrectly as a result of a coding error affecting Tables 1 and 2, Equation 7 (right formulae), and Figure 2a. The following have since been corrected, and this version may be considered the authoritative version of record. In Tables 1 and 2 (Phase column): 27.83 was changed to 10.69, −83.26 was changed to 73.81, and 128.68 was changed to −43.01. In the acknowledgments, the following statement was added: We thank B. Giese for pointing out the problem of the phase calculation and B. Noyelles for an independent check.